RSC Advances

ROYAL SOCIETY OF CHEMISTRY

www.rsc.org/advances

Alumina Coating on 5 V Lithium Cobalt Fluorophosphates Cathode Material for Lithium Secondary Batteries – Synthesis and Electrochemical Properties

S. Amaresh[a], K. Karthikeyan[a], K.J. Kim[a], K.S. Nahm[b,c,d,*], Y.S. Lee[a,*]

[a]Faculty of Applied Chemical Engineering, Chonnam National University,

Gwangju 500-757, Korea

[b]Department of Energy Storage and Conversion Engineering, [c]R&D Education Center for Fuel Cell Materials & Systems, and [d]Department of Semiconductor and Chemical Engineering, Chonbuk National University, Jeon-ju 561-756, Korea

Abstract

High voltage cathode material, Li_2CoPO_4F was successfully synthesized and coated with various amounts of Al_2O_3 for enhanced electrochemical performance. X-ray diffraction data revealed that the unit cell had orthorhombic structure with *Pnma* space group. An initial discharge capacity of ~127 mAh g^{-1} was obtained between 2 and 5.1 V. The capacity retention, ratio of discharge capacity at 15th cycle to that at 1st cycle, at current rate of C/2 was increased from 53 % for pristine sample to 73 % for 1 wt% Al_2O_3 coated Li_2CoPO_4F. Cyclic voltammetry and charge/discharge studies showed an increased operating voltage for Li_2CoPO_4F after Al_2O_3 coating. Electrochemical impedance spectroscopy result suggested a

* Corresponding author.

Tel. & Fax : +82 62 530 1904, E-mail : leeys@chonnam.ac.kr (Y.S. Lee).

Tel : +82-63-270-2311, Fax : +82-63-270-3909, E-mail : nahmks@jbnu.ac.kr (K.S. Nahm)

reduction in charge transfer resistance in as-prepared samples. Moreover, the reduction in irreversible capacity loss, defined as the difference between charge capacity and discharge capacity of the same cycle, in the initial cycle suggested a decrease in electrolyte oxidation after coating process. A uniform amorphous layer of Al_2O_3 coating of ~3 nm thickness protected the surface of Li_2CoPO_4F during high voltage operation.

Key words: *Al_2O_3; coating; Li_2CoPO_4F; XPS; cathode; lithium battery*

Introduction:

Lithium ion battery has been established as one of the major energy storage devices in past two decades, ever since the commercialization of $LiCoO_2$ cathode by SONY. Applications utilizing lithium ion batteries as power source ranges from small electronic devices to fully electrify commercial passenger vehicles at present and this trend will be extended to multi-utility and heavy vehicles in future. The increasing demand for energy storage guided researchers to explore materials that are capable of storing more lithium per formula unit and thereby increasing the discharge capacity of the cathode materials.[1-3] The fluorophosphate family of cathodes has attracted recent interests due to the presence of highly stable PO_4^{3-} ions in the crystal lattice which is responsible for the consistent performance of batteries in both low and high temperature environments than the corresponding oxides.[4,5] The cobalt based fluorophosphate Li_2CoPO_4F was less explored, since the operating voltage is believed to be very high > 5 V, but has a high theoretical gravimetric and volumetric specific energy of 589 Wh kg^{-1} and 1928 Wh L^{-1}, respectively.[6] Since its introduction by Okada *et al*,[7] the lithium cobalt fluorophosphates (Li_2CoPO_4F, LCPF) was evaluated by various research groups.[8,11-13] The inducting effect of phosphate ion combined with the highly electronegative F^- ions can be helpful in increasing the thermal and chemical stability. Hence,

it is believed that there is a high possibility of Li_2CoPO_4F cathode material to be used in next generation batteries, which can satisfy energy needs of various applications.

A complete structural elucidation by precession electron diffraction experiments showed that Li_2CoPO_4F has orthorhombic structure as that of parent olivine phosphate $LiCoPO_4$, but with corner shared CoO_4F_2 octahedral chains interconnected into a 3D framework by PO_4 tetrahedral units. The lithium ions are located along the channels formed by the framework structure and migrate along the *b*-axis during intercalation.[8] Lithium cobalt fluorophosphate also shared a similar structure as that of other fluorophosphates namely, Li_2NiPO_4F,[9] and $Li_{1.75}Ni_{0.75}Fe_{0.25}PO_4F$.[10] The difficulty in synthesizing pure phase of Li_2CoPO_4F by solid state method was demonstrated earlier.[12,14] Li_2CoPO_4F formed a metastable phase and hence it is highly susceptible for breaking down into $LiCoPO_4$ and LiF along with the formation of impurities like Li_3PO_4, CoP_3, and CoO. There was also an attempt to synthesis pure Li_2CoPO_4F phase without forming intermediate $LiCoPO_4$ phase and to cut down one step of preparation process, but the resultant material had mixture of both $LiCoPO_4$ and Li_2CoPO_4F phases marked with some of the impurities as said above.[11,12] In spite of the complexity involved in the synthesis methodology, the electrochemical activity of Li_2CoPO_4F material was confirmed by quasi reversible voltage profiles by Okada *et al*,[7] and was determined that the intercalation phenomenon in Li_2CoPO_4F was a single phase reaction unlike $LiCoPO_4$ that undergoes two phase reaction. The maximum discharge capacity for Li_2CoPO_4F by solid state method was 109 mAh g^{-1}; obtained by cycling between 2 and 5.5 V was demonstrated by Wang *et al*,[10] using a sulfone based electrolyte, whereas the iso-structural Li_2NiPO_4F exhibited severe capacity fading even against high voltage stable sebaconitrile based electrolyte.[40] An unconventional spark plasma sintering technique for synthesizing phase pure LCPF ended up with large particles of size greater than 5μm and performance close to those reported in the literature.[13] In our recent experiments, we

successfully synthesized Li_2CoPO_4F materials by two step process involving the synthesis of $LiCoPO_4$ phase initially, followed by the introduction of LiF into the crystal lattice of $LiCoPO_4$ to form Li_2CoPO_4F. The critical role of synthesis duration and temperature involved during the formation of Li_2CoPO_4F phase was elucidated. The discharge capacity obtained in our experiments was 132 mAh g^{-1} between 2 and 5.1 V. The obtained capacity was superior to the results obtained by solid state synthesis available in the literature and the capacity retention was hindered by the heavy decomposition of electrolyte.[14] However, the materials had to be focused more to improve the discharge capacity close to the theoretical value of 287 mAh g^{-1} for two lithium ion extraction and to establish a new class of 5 V cathodes for lithium secondary batteries.

One way to improve the electrochemical activity of cathode materials is to introduce coating over the surface of the cathode materials, so that the additional layer protects the electrode material from hazardous reaction products obtained during the charge-discharge process. The decomposition of electrolyte in high voltage operation creates a highly acidic environment near the surface of electrode materials, which is responsible for metal ion dissolution and decrease in inherent potential of cathode active material. This, in turn, provides fewer sites for intercalation as the structure of cathode material is altered. Metal oxide coating over the surface of electrode can form a protective layer by covering active sites of electrode material that acts as a catalyst with acidic HF, which is formed as the decomposition product of $LiPF_6$ with the trace amount of water present in electrolyte and cell components.[15-17] On the other hand, surface coatings can form solid solution on the surface and stabilizes structure of cathode material with the help of a highly lithium ion conducting layer. A stable solid electrolyte interface is thus formed and allows for smooth electrochemical interaction between the electrodes.[18-20] Improved thermal stability of surface coated materials can be due to the factors like increase in surface area and ionic

conductivity.[21] The oxide counterpart of cobalt i.e. $LiCoO_2$, when treated with Al_2O_3 coating, showed improved electrochemical performance such as rate capability, high voltage charge-discharge characteristics, thermal stability and capacity retention. For example, Cho *et al*[19] reported that the capacity of $LiCoO_2$ could be improved, with aluminium oxide surface coating, to 170 mAh g^{-1} when cycled between 2.75 and 4.4V. A very minimal capacity loss of ~5% was observed and the enhanced performance was related to the reduced reaction between the cobalt ions during charging with the acidic HF in the electrolyte. In addition, Al_2O_3 coated $LiCoO_2$ performed much better than the SnO_2 surface modified active materials in terms of capacity and retention.[20]

In this regard, Al_2O_3 was selected for coating over the surface of solid state synthesized Li_2CoPO_4F. The coating ratio of 1, 3 and 5 wt% of initial starting materials were fixed with a moderate post annealing temperature. To the best of our knowledge, this is the first attempt in employing Al_2O_3 to improve electrochemical properties on framework cobalt fluorophosphate cathode materials to be cycled above 5V. The preliminary results showed an improvement in capacity retention at high current rates and improved cycle stability for Li_2CoPO_4F cathode that can be assigned to a thin layer of surface coating.

Experimental

Li_2CoPO_4F powder was synthesized by conventional two step solid state method as reported in our earlier study.[14] Briefly, the starting materials of lithium hydroxide monohydrate (Junsei, Japan), cobalt (II,III) oxide (Alfa Aesar, USA) and ammonium phosphate dibasic (Sigma–Aldrich, USA) were stoichiometrically weighed and mixed using planetary ball mill for 3 hrs at 400 rpm using acetone as medium. The resultant mixture was dried at 60 ^oC until the acetone gets evaporated, pelletized, and annealed at 400 ^oC and 800 ^oC for 10 hrs in air atmosphere to yield $LiCoPO_4$. The obtained $LiCoPO_4$ was reground

thoroughly with LiF (Wako, Japan) and was heated under argon atmosphere at 700 ^{o}C. The powder was quenched to room temperature after 1.5 hrs of heat exposure. About 10 wt% excess lithium hydroxide monohydrate was used to compensate the lithium loss during high temperature treatment. The heating time for final sintering was optimized such that the decomposition of Li_2CoPO_4F was avoided and thus a phase pure Li_2CoPO_4F is prepared.

To coat Al_2O_3 on the surface of Li_2CoPO_4F, the acetate salt of aluminium, namely dihydroxy aluminium acetate (Sigma–Aldrich, USA) was firstly dissolved in water and stirred constantly at 50 ^{o}C for 2 hrs. The synthesized Li_2CoPO_4F powder was surface prepared by sonication for 1 hr at 50 ^{o}C in water. Li_2CoPO_4F mixture was added to coating solution such that the total amount of metal oxide to be coated were exactly 1, 3, and 5 wt% of the initial starting materials. The mixture was dried in an oven at 120 ^{o}C, heat treated at 500 ^{o}C for 5 h in air atmosphere and finally reground before being used for various studies.

The formation of uncoated and Al_2O_3 coated Li_2CoPO_4F materials were confirmed by X-ray diffractometer (XRD, Rint 1000, Rigaku, Japan) using Cu Kα radiation (λ = 1.54056 Å) between 5 and 55^{o} at 0.02^{o} steps and 0.3s step time. The morphological characteristics of the samples were studied using field emission scanning electron microscope (FE-SEM, S-4700, Hitachi, Japan) equipped with a Robinson-type backscattered electron detector and with an Energy-dispersive X-ray spectroscope (EDAX) attachment and Transmission electron microscopy (TEM, TECNAI, Philips, Netherlands) operated at 200 keV. The X-ray photoelectron spectroscopy (XPS, Multilab2000, VG, UK) operational with an electron energy analyzer (Alpha 110 analyzer) equipped with a non-monochromatic Mg Kα radiation of 1253.6 eV was used to analyze the composition of prepared samples. The measurement was carried out under ultra high vacuum. The spectrometer was calibrated using the C 1s line of binding energy 285.0 eV of graphitic carbon. The stoichiometry of the sample was analyzed using Inductively Coupled Plasma Atomic Emission Spectrometer (ICP, OPTIMA

4300 DV). A 4 mg pellet was used for Fourier transform infrared spectroscopy (FTIR, IRPresitge-21, Shimadzu, Japan) between 4000 and 500 cm^{-1} with a resolution of 4 cm^{-1}. Electrochemical characterizations of all the synthesized materials were performed using a CR2032 coin cell, fabricated in a glove box under controlled atmosphere. The cell consisted of synthesized material as cathode and metallic lithium as anode. A polypropylene separator soaked in the electrolyte containing 1M $LiPF_6$ dissolved in EC:DMC (1:1 v/v) was sandwiched between the electrodes. The cathodes were prepared by mixing active material, ketzen black (KB) and teflonized acetylene black (TAB) (weight ratio 76:12:12) into a slurry. The slurry was then carefully spread over a nickel mesh current collector, followed by drying at 110 ^oC for 4 hrs before being used in the cell. Galvanostatic charge/discharge tests with a battery tester (WBCS 3000, Won-A-Tech, Korea) was used to evaluate the electrochemical performance of uncoated and Al_2O_3 coated Li_2CoPO_4F cathode materials. Electrochemical impedance spectroscopy (EIS) and cyclic voltammetry (CV) studies were performed using an electrochemical work station (SP-150, Biologic, France) at room temperature on freshly prepared cells. The EIS spectra were measured between the frequency range 100 kHz to 100 mHz using an applied current amplitude of 100 μA at open circuit potential, while the CV was tested at a scan rate of 0.1 mV s^{-1} between the operating voltage of 2 and 5.1 V with lithium being both counter and reference electrode.

Results and discussion

The structural characteristics of synthesized uncoated and Al_2O_3 coated Li_2CoPO_4F materials were analyzed by X-ray diffraction studies and the results are shown in figure 1(a). Bragg reflections for uncoated and coated samples were identical, which indicated that coating does not alter inherent structure of Li_2CoPO_4F powder. These Bragg reflections were indexed on Orthorhombic unit cell having *Pnma* space group and agreed well with JCPDS

card #56-1493. Furthermore, XRD profiles of coated samples did not show diffraction lines of Al_2O_3 phase; hence the coating is believed to be thin or amorphous forms. Heat treatment temperature after coating was fixed at 500 ^oC because the phase formation for Li_2CoPO_4F sample was 700 ^oC, which may result in deformation into $LiCoPO_4$ and LiF when overheated.[11,13,14] It is speculated that there may be solid solution formation during the post heat treatment process after coating by the tendency of cobalt ions to move through the coating layer and interact with aluminum ions. However, the formation of this solid solution will be on surface and does not penetrate into the bulk of active material. A highly sensitive surface analysis like XPS will be helpful in checking the formation of solid solution between aluminum and cobalt ions, which will be dealt in the later part of this article. In the mean while, the P/F ratio was determined by EDAX and found to be 0.17 : 0.16; this value is consistent with the stoichiometric ratio of P/F = 1, which is the same as that of the Co/F ratio. The Li/Co ratio of 2.02 was observed from ICP analysis of the sample.

Typical internal vibrations i.e., v_1–v_4 of rigid tetrahedral polyanion group PO_4^{3-} was observed from FTIR spectra of uncoated and Al_2O_3 coated Li_2CoPO_4F (figure 1(b)). The basic functional group is not altered even after coating and subsequent post treatment at 500 ^oC as evident from the indistinguishable IR spectra. The bands in higher wave number region from 800-1250 cm^{-1} confirmed presence of stretching mode of $(PO_4)^{3-}$ ions well apart from the bending vibrations exhibited at 630 and 585 cm^{-1}. The symmetrical splitting of 1072 and 1030 cm^{-1} of the first stretching vibration can be interpreted for more equally strengthened P-O bonds. This PO_4 formed a tetrahedral unit and coordinated the octahedral CoO_4F_2 units share common edges running an infinite chain along b-axis to form a 3D framework. The tunnel running along the *b*-axis as a result of the framework structure is occupied by the Li atoms for insertion/extraction.[8] The bands seen at 1633 and 3440 cm^{-1} represented bending and stretching vibrations of hydroxyl group in water molecules present in the samples.

Figure 2 shows SEM images of uncoated and Al_2O_3 coated Li_2CoPO_4F samples with particles in 50-120 nm size range. The particles had strong agglomeration and the presence of intermediate void spaces help electrolyte to reach the inner layer of agglomerated particle. The surface of coated samples got brighter with increase in coating material content. This increase in brightness was due to charge accumulation as the electron beam comes into contact with coating material. It could be seen that the coating appear to be uniform at low concentration i.e., 1 wt%, while there was accumulation of small particles over the surface of Li_2CoPO_4F powder that can be distinguished with the brightness of Al_2O_3 particles. The coating mechanism was believed to have two steps: (i) formation of small spherical particle over the surface of core material and (ii) the subsequent heat treatment helped in formation of uniform layer over the entire surface of core material. A continuous layer of coated material was clearly seen in high resolution TEM picture of 1 wt%-Al_2O_3 coated Li_2CoPO_4F sample with a coating thickness of ~3 nm (inset in figure 2(b)), while uncoated Li_2CoPO_4F showed lattice fringes until the surface of particle (inset in figure 2(a)) that implied absence of coating layer. The inset of figure 2(b) exhibited two distinct regions; randomly oriented crystals with lattice fringes in the core that exemplified Li_2CoPO_4F and an outer amorphous region signified Al_2O_3 coating layer. Thus it was confirmed that the coating layer is amorphous and hence it does not show up in the data obtained using XRD. The increase in content of coating material has led to accumulation of globule over surface of Li_2CoPO_4F material, which on further heat treatment got aggregated (figure 2(c) and 2(d)). The formation of aggregates would block parent materials and can reduce active area for electrochemical insertion/ extraction reaction. Moreover, presence of additional globules between Li_2CoPO_4F active materials could reduce particle to particle contact and thereby could affect charge/discharge characteristics. This phenomenon can be held responsible for variable electrochemical performance of Li_2CoPO_4F and hence a lower coating content is suggested for uniform

coating.

The voltage profiles of uncoated and Al_2O_3 coated cells cycled between 2 and 5.1 V were presented in figure 3. An initial discharge capacity of ~127 mAh g^{-1} was obtained for uncoated Li/Li_2CoPO_4F cell, while a discharge capacity of 125, 118, and 118 mAh g^{-1} were observed for cells containing 1, 3, and 5 wt% Al_2O_3 coated Li_2CoPO_4F cathode, respectively. High voltage operation usually led to electrolyte decomposition, formation of reactive byproducts of decomposition and a subsequent reaction with active materials, oxygen loss by evolution and a passive film formation near the surface of active material. As a result, electrochemical activities of electrode materials gets decreased; resistance is increased and lithium ion diffusivity is lowered.[22,23] The coating layer forms a barrier between highly reactive decomposition products like acidic HF and surface of cathode material, which is protecting the cathode surface from acid attack and further degradation.[24,25] This phenomenon can be examined by charge-discharge characteristics of uncoated and Al_2O_3 coated Li_2CoPO_4F cells. A charge capacity of 247 mAh g^{-1} was obtained for uncoated Li_2CoPO_4F cell. However, the charge capacities of Al_2O_3 coated Li_2CoPO_4F cells decreased to a maximum of ~ 32 % to ~170 mAh g^{-1} for 3 and 5 wt% samples and ~190 mAh g^{-1} for 1 wt% coating content. The decrease in charge capacity can be taken as favorable for less exposure of active materials to electrolyte decomposition products and a significant decrease in irreversible capacity loss can be accounted. On the other hand, the decrease in charge capacity for 3 and 5 wt% samples are quite high compared with that of uncoated sample, probably due to the high coating content that hindered interaction between active materials, which decreased the rate of lithium ion diffusion and reduced the intercalation reaction.

The charge/discharge curves had a continuous differential nature, unlike a flat voltage window in the case of parent $LiCoPO_4$ phase, hence Li_2CoPO_4F has a single phase reaction. An increase in operating voltage plateau to a maximum of 100 mV was observed

between uncoated and Al_2O_3 coated Li_2CoPO_4F cells. The superior resistance of Al_2O_3 against the decomposition products of electrolyte has led to the increased electrochemical activity of Li_2CoPO_4F material. Furthermore, transformation of surface impurity phases in uncoated sample during post treatment after Al_2O_3 coating may be responsible for improved charge/discharge characteristics. The uncoated material also suffers from inaccessible lithium site, wherein among the identified three lithium sites, only two are readily accessible while the third lithium is less mobile due to the shortest distance between nearest oxygen/fluorine atoms.[8] In spite of delivering a high charging capacity, the discharge capacity achieved corresponds to a single lithium insertion reaction. Hence, the upper cut off voltage of 5.1 V is not sufficient for extracting two lithium ions present in framework Li_2CoPO_4F cathode materials. However, it was found that our attempt to charge Al_2O_3 coated Li_2CoPO_4F above 5.1 V resulted in severe irreversible capacity loss and subsequent influence in cycle characteristics. So, the upper cut-off voltage was restricted to be 5.1 V throughout the study.

Capacity *vs*. cycle number plot of uncoated and Al_2O_3 coated Li_2CoPO_4F sample cycled between 2 and 5.1 V at C/2 rate were presented in figure 4. The cycle life data of uncoated Li_2CoPO_4F sample (figure 4(c)) showed an initial capacity of 101 mAh g^{-1} and degraded upon cycling with capacity loss of ~53 % after 15 cycles. The coated samples provided much better results in terms of initial capacity and capacity retention rate during cycling. For instance, 1 wt% Al_2O_3 coated Li_2CoPO_4F material delivered an initial capacity of 106 mAh g^{-1} and retained 79 mAh g^{-1} after 15 cycles. This accounts to capacity retention of 73 %, which is about 20 % increase in retention rate. Even though 3 and 5 wt% Al_2O_3 coated samples exhibited a higher initial capacity of 112 and 108 mAh g^{-1}; the respective capacities decreased to 72 and 68 $mAhg^{-1}$ after 15 cycles with capacity retention of ~ 63 %. The presence of uneven coating layer over Li_2CoPO_4F and particle accumulation as coating ratio increased can be responsible for capacity degradation in the case of 3 and 5 wt% coated

samples. Increased particle accumulation forms a thick inactive layer of oxides which allowed less lithium to diffuse through. There is also possible exposure of active material in the case of 3 and 5 wt% coated samples. Over all, the Al_2O_3 coating has increased the ability of Li_2CoPO_4F to retain discharge capacity at high operating voltages.

In addition, noticeable improvement in surface characteristics can be observed from change in nature of charge/discharge profile. The first and tenth cycle of cells containing uncoated and Al_2O_3 coated Li_2CoPO_4F samples were presented in figure 4(a) and 4(b). The charge/discharge profiles showed fast discharge capacity fading for pristine Li_2CoPO_4F, which may due to surface erosion caused at high voltage in the presence of acidic decomposition species from electrolyte. In contrary, Al_2O_3 coated samples exhibited a similar nature of voltage profile during the tenth cycle as that of the first cycle, representing a stable surface due to the presence of Al_2O_3 coating. The capacity fading in case of Li_2CoPO_4F is related to high operating voltage, instability, oxidation of electrolyte at higher voltage, and possibly metal dissolution upon cycling due to reaction between acidic electrolyte decomposition products and surface of active material. The surface coating by Al_2O_3 helped Li_2CoPO_4F to refrain from later reasons and hence, stabilized exterior layer of Li_2CoPO_4F by increasing lithium ion diffusion. There are many reports on formation of AlF_3 layer from reaction of Al_2O_3 with acidic HF.[26] Most of the oxide based coating materials transformed into metal fluorides and stabilized interface between active material and electrolyte.[17,23] It is also believed that formation of metal fluorides is beneficial in improving the cycle life of transition metal based cathode materials. A similar phenomenon is also speculated for the present case mainly because of high voltage operation i.e., above 5 V *vs*. Li wherein the commonly used electrolyte decomposes severely. In any case, improvement in cell characteristics can be achieved only with a thin protective coating layer, which can act as HF scavengers and restricts surface corrosion of active materials.

The CVs of cell with uncoated and Al_2O_3 coated active materials were tested and the results are shown in figure 5. The CV curves of all samples exhibited a reduction peak at ~ 4.6 V and an incomplete oxidation peak at 5 V, denoting that the redox reaction corresponds to Co^{3+}/Co^{2+} process and two lithium ions cannot be extracted until 5.1 V. The broad peak observed in redox process due to two steps of lithium extraction at different crystal lattice sites and insertion during reduction. It is worth noting here that the oxidative and reductive area decreased with increase in coating content. The pristine sample exhibited a maximum current response during oxidation, which is the same as the additional charging capacity due to electrolytic oxidation observed in charge/discharge studies. There was a shift in reduction potential between uncoated and coated samples of *c.a.* 70 mV, as seen in the inset of figure 5. The heat treatment after Al_2O_3 coating resulted in the easy synthesis of pure Li_2CoPO_4F phase with no reflection from crystalline Al_2O_3 phase. However, the uncoated sample had impurities ~32^o in XRD corresponding to Li_3PO_4 phase. The phase stabilization during post treatment after coating resulted in pure phase and can be responsible for change in reduction peak potential observed in CV. These results can be correlated well with charge/discharge data obtained within the same potential range.

Figure 6 shows the experimental and fitted data obtained from electrochemical impedance spectroscopy for uncoated and coated samples at open circuit potential. The results of all cells exhibited a semicircle at high-medium frequency region and an inclined line at approximately 45^o to real axis corresponding to Warburg impedance associated with lithium ion diffusion in the electrode. The semicircle is accounted for combined effect of resistance due to SEI film formed over particle surface, contact resistance between particles and charge transfer resistance (R_{ct}) along with corresponding capacitance. The starting point of semicircle at high frequency region represented electrolytic resistance (R_s). The R_{ct} of coated materials were in the order of 1 wt% < 3 wt% < 5 wt% i.e., 8, 10, and 20 Ω,

respectively. Therefore, electrochemical performance of cathode materials was affected in the same order as evidenced from charge/discharge studies. EIS was also used to study the lithium ion diffusion coefficient for understanding the reason behind increase in performance of coated sample using formula given elsewhere.[27,28] Briefly, the diffusion co-efficient of Li ions for Li_2CoPO_4F can be calculated from the following equation: $D_{Li}^{+} = (1/2)\ [(V_M/FA\sigma)\ (\delta E/\delta x)]^2$, where V_M, F, A and σ denote the molar volume (m^3), the Faraday's constant, the surface area of the electrode, and Warburg constant, respectively. The Warburg constant can be obtained from the slope of Z' vs $\omega^{-1/2}$ or -Z" vs $\omega^{-1/2}$ plots (ω is the angular frequency). δE/δx can be obtained from the slope of galvanostatic discharge curve. Accordingly, the calculated lithium diffusion coefficient can be found in table 1. It is evident that diffusion of lithium ion got increased after coating and also the maximum was found for 1 wt% Al_2O_3 coated sample. It is interesting to note that a thin layer of Al_2O_3 formed over the surface of Li_2CoPO_4F enhanced its performance, even though Al_2O_3 is an electrically insulating material. The insulating coating layer can reduce contact between particles and electrolyte, thereby, deteriorate charge transfer between active material and current collector, which lead to increase in charge transfer resistance. But, the results are different in Al_2O_3 coated Li_2CoPO_4F case. There is a decrease in R_{ct} for 1 wt% Al_2O_3 coated sample when compared with uncoated sample and hence, lower impedance is related to lower polarization and improved performance of Li_2CoPO_4F cell. Hence, it can be concluded that Al_2O_3 coating affects the kinetics of lithium diffusion and charge transfer resistance during cycling, provided the thickness of coating should be controlled.

It is well known that XPS analysis is an efficient technique in interfacial composition analysis of lithium ion batteries.[29-32] Recently, surface chemistry of coated cathode materials and the reactions between active surface and electrolyte was popularized. Surface coating on cathode material has worked by inhibiting metal dissolution, reducing electrolyte degrading

component, and forming an active lithium ion conducting layer like Li_3PO_4 layer.[33,34] In the present investigation, however, analysis is limited to surface composition of uncoated and Al_2O_3 coated Li_2CoPO_4F cathode materials. XPS spectra presented in figure 7(a) is very much important, because it shows Al 2p and Li 1s spectra. Aluminum is detected in all three coated materials, while pristine material does not have any trace for Al atoms. The atomic percentages of aluminum were 3.24, 6.95, and 11.91% over the surface of 1, 3, and 5 wt% coated samples, respectively. The Al 2p spectra consisted of a single peak at 74±0.07 eV, which can be assigned to aluminum atoms in oxide environment.[35] The possibility of solid solution formation by coexistence of Al and Co atoms on surface layer cannot be ruled out. Since surface coating over a variety of cathode materials have led to solid solution formation, it can be responsible for improvement in electrochemical stability of active material. In view of the fact that solid solution development takes place during calcination step after coating, a noticeable change in emission characteristics is expected at least at high coating content. Verdier *et al*[34] have noticed an over lapping peak at lower binding energy of Al 2p with the satellite peak of Co 3p at 73.4 eV for solid solution formation which contained an Al/Co ratio of 0.7. This shift in peak position for Al 2p was not observed in the case of Al_2O_3 coated Li_2CoPO_4F samples. Moreover, the area of Al 2p peak increased with coating content, while the area of Co 3p peak (at BE of 61 eV) were almost the same in all samples. Hence, the calcination step in case of Al_2O_3 coated Li_2CoPO_4F does not alter coating composition and Al atoms does not get involved in solid solution formation. On the other hand, Li 1s spectra were observed at 55.2±0.1 eV for both pristine and coated samples that corresponds to +1 oxidation state of lithium. This binding energy is lesser than that of lithium ion in LiF (~56 eV) or $LiPF_6$ (~56.8 eV) environments.

The cobalt ions were also observed through Co 2p spectra as shown in figure 7(b). The Co 2p spectra consists of two peaks representing Co $2p_{1/2}$ and Co $2p_{3/2}$ binding energies

with a peak ratio of 1/2. The main peak Co $2p_{3/2}$ is located at 781 ±0.1 eV and Co $2p_{1/2}$ peak can be found at 797 ±0.1eV for all the samples. Each of these peaks were followed by a satellite peaks at approximately ~9 eV apart. These peak positions along with satellite peak can be assigned to +2 oxidation state of cobalt in an oxide environment.[36] There is also a shift in Co $2p_{1/2}$ peak position where a closer satellite is observed, which indicated a different interaction unlike that of parent $LiCoPO_4$.[37] The Al_2O_3 coated materials did not show shift in peak position and were identical with uncoated material, indicating that coating did not alter the intrinsic property of the Li_2CoPO_4F irrespective of coating content and solid solution feature could be eliminated. Additionally, the cobalt redox couple was checked in a partially charged electrode (at 5.05V). The Co 2P XPS spectra from figure S1 (Supporting Information) demonstrated a reduction in binding energy of the Co 2P peaks to about 1.5±0.1eV denoting the change in valence state of cobalt ion during charging, thus confirming the activity of redox couple.

The O 1s photoemission line, given in figure 7(c), exhibited a single broad peak at 531±0.1 eV for all samples. There is no peak shift observed for all coated samples, hence Al_2O_3 interaction can be assumed to be within the observed region. The peak position for O 1s was different from that observed for $LiCoO_2$,[37] but coincides with olivine $LiCoPO_4$ compound representing an oxidation state of –2 for oxygen.[38,39] This peak is very strong, while two weak peaks at 529.9 eV and 532.2 eV were observed during deconvolution that signified the existence of strong covalence with cobalt and interaction of oxygen with hydrogen, as in water observed from FTIR spectrum (figure 1(b)), respectively. The P 2p (figure 7(d)) spectra specified a strong emission line at 133.1±0.1 eV, which denoted phosphorous in PO_4^{3-} poly anion surroundings has +5 oxidation state. Furthermore, there are no additional weak peaks observed in P 2p, when deconvoluted, indicating strong bonding in phosphate anion. Lastly, the F 1s spectral line showed a strong peak at 684.3 ±0.1 eV (figure

7(e)). The F 1s spectra does not show peak corresponding to unreacted LiF nor C–F interaction, which are characterized by the respective peaks at 685 and 687.7 eV. The absence of these peaks denoted a complete reaction of LiF to form crystalline Li_2CoPO_4F during two step solid state process. Moreover, the P 2p and F 1s spectra are analogous for uncoated and Al_2O_3 coated Li_2CoPO_4F samples. Therefore, it is confirmed that coating and post treatment after coating process does not alter the structural characteristics of Li_2CoPO_4F cathode material.

The assessment of the XPS spectrum (see Supporting information, figure S1) of the partially charged (at 5.05V) 1wt% Al_2O_3 coated Li_2CoPO_4F electrode provided insight into the occurrence of electrolyte decomposition products even at the initial cycle. The C 1s spectra represents the presence of Carbon together with the organic by-products like C-O (287 eV) and COO (289 eV) groups.[34] In addition, the F 1s spectra depicts the presence of $Li_xPO_yF_z$ (686 eV) compound.[34,41] On the other hand, nano-Al_2O_3 particles was proven to be HF scavenger in the case of 1M $LiPF_6$ (EC:DMC, 1:1, v/v) electrolyte for high voltage $LiCoO_2$ cathode material.[42] The formation of AlF_3 in reaction with the HF, which is the reaction product of the moisture present in the electrolyte, was responsible for the improvement in capacity retention. The detailed reaction mechanism for the formation of HF and AlF_3 can be found elsewhere.[42] Consequently, the Al_2O_3 coating over the surface of Li_2CoPO_4F gets converted to AlF_3 layer. The presence of a peak at 77±0.1 eV[43] in Al 2P XPS spectrum (figure S1) for the partially charged 1wt% Al_2O_3 coated Li_2CoPO_4F electrode corroborated the existence of AlF_3. Upon charging to a higher voltage (> 5.0V), the rate of electrolyte decomposition is increased and thus favored the conversion of Al_2O_3 to AlF_3 at the initial charging itself. The AlF_3 layer emerges as a protective layer against acidic decomposition products and restricts the exposure of active material. The reaction between transition metal at de-lithiated state with the electrolyte component can be restricted or

reduced with the help of the physical barrier (coating layer) at the cathode active material. Therefore, electrochemical properties like operating voltage, charge-discharge characteristics, rate performance and capacity retention had a positive impact in the case of metal oxide coated Li_2CoPO_4F cathode materials. It is equally important to mention here that the optimization of content of the coating is necessary because higher coating content leads to decrease in electrochemical characteristics.

Conclusion

Surface modification by Al_2O_3 had effectively improved the electrochemical characteristics of Li_2CoPO_4F cathode material. An improvement in charge/discharge characteristics and capacity retention were observed. The Al_2O_3 layer was found to be amorphous and thin over crystalline Li_2CoPO_4F surface. There is no solid solution formation in the as prepared Al_2O_3 coated Li_2CoPO_4F materials. The formation of AlF_3 during the initial charge cycle was determined using ex-situ XPS analysis. Hence, Al_2O_3 coating served as a protecting layer between electrolyte and cathode surface. This helped in protecting the cathode material from adverse reactions with acidic species from electrolyte oxidation. The possible metal dissolution can be reduced in the presence of coating, which improved capacity retention through enhanced lithium ion diffusion and reduced charge transfer kinetics.

Acknowledgements

This research was supported by Basic Science Research Program through the National Research Foundation of Korea (NRF) funded by the Ministry of Education(No. 2013R1A1A2012656). This work was also partially supported by the Human Resources

Development program (No. 20114030200060) of the Korea Institute of Energy Technology Evaluation and Planning (KETEP) grant funded by the Korea government Ministry of Trade, Industry and Energy.

References

1 M. Armand and J.-M. Tarascon, *Nature*, 2008, **451**, 652.

2 V. Etacheri, R. Marom, R. Elazari, G. Salitra and D. Aurbach, *Energy Environ. Sci.*, 2011, **4**, 3243.

3 M. S. Whittingham, *Chem. Rev.,* 2004, **104**, 4271.

4 J. Jiang and J.R. Dahn, *Electrochem. Commun.*, 2004, **6**, 39.

5 G. Hautier, A. Jain, S. P. Ong, B. Kang, C. Moore, R. Doe and G. Ceder, *Chem. Mater.*, 2011, **23**, 3495.

6 T. Mueller, G. Hautier, A. Jain and G. Ceder, *Chem. Mater.*, 2011, **23**, 3854.

7 S. Okada, M. Ueno, Y. Uebou and J-i. Yamaki, *J. Power Sources*, 2005, **146**, 565.

8 J.Hadermann, A. M. Abakumov, S. Turner, Z. Hafideddine, N. R. Khasanova, E. V. Antipov and G. V. Tendeloo, *Chem. Mater.*, 2011, **23**, 3540.

9 M. Gemmi, X. D. Zou, S. Hovmöller, A. Migliori, M. Vennström and Y. Andersson, *Acta Crystallogr.*, 2003, **A59**, 117.

10 D.Wang, J. Xiao,W. Xu, Z. Nie, C. Wang, G. Graff and J.-G. Zhang, *J. Power Sources*, 2011, **196**, 2241.

11 N. R. Khasanova, A. N. Gavrilov, E. V. Antipov, K. G. Bramnik and H. Hibst, *J. Power Sources*, 2011, **196**, 355.

12 N.V. Kosova, E.T. Devyatkina and A.B. Slobodyuk, *Solid State Ionics*, 2012, **225**, 570.

13 E. D. Botto, C. Bourbon, S. Patoux, P. Rozierb and M. Dolle, *J. Power Sources*, 2011, **196**, 2274.

14 S. Amaresh, G. J. Kim, K. Karthikeyan, V. Aravindan, K. Y. Chung, B. W. Cho and Y. S. Lee, *Phys. Chem. Chem. Phys.*, 2012, **14**, 11904.

15 Z. Chen, Y. Qin, K. Amine and Y.-K. Sun, *J. Mater. Chem.*, 2010, **20**, 7606.

16 Z. H. Chen and J. R. Dahn, *Electrochem. Solid-State Lett.*, 2003, **6**, A221.

17 Y. K. Sun, Y. S. Lee, M. Yoshio and K. Amine, *Electrochem. Solid-State Lett.*, 2005, **5**, A99.

18 J. Cho, Y.J. Kim and B. Park, *J. Electrochem. Soc.*, 2001, **148**, A1110.

19 J. Cho, Y.J. Kim and B. Park, *Chem. Mater.*, 2000, **12**, 3788.

20 J. Cho, C.S. Kim and S.I. Yoo, *Electrochem Solid-State Lett.*, 2000, **3**, 362.

21 S. Oh, J.K. Lee, D. Byuna, W. Cho and B.W. Cho, *J. Power Sources*, 2004, **132**, 249.

22 P. Arora, R. E. White and M. Doyle, *J. Electrochem. Soc.*, 1998, **145**, 3647.

23 A. R. Armstrong, M. Holzapfel, P. Novák, C. S. Johnson, S.-H. Kang, M. M. Thackeray and P. G. Bruce, *J. Am. Chem. Soc.*, 2006, **128**, 8694.

24 Z. Chen, Z. Lu and J. R. Dahn, *J. Electrochem. Soc*., 2002, **149**, A1604.

25 J. M. Zheng, Z. R. Zhang, X.B. Wu, Z. X. Dong, Z. Zhu and Y. Yang, *J. Electrochem. Soc*., 2008, **155**, A775.

26 S.-T. Myung, K. Izumi, S. Komaba, Y.-K.Sun, H. Yashiro and N. Kumagai , *Chem. Mater*., 2005, **17**, 3695.

27 J. Xie, K. Kohno, T. Matsumura, N. Imanishi, A. Hirano, Y. Takeda and O. Yamamoto, *Electrochim. Acta*, 2008, **54**, 376.

28 X.H. Rui, N. Ding, J. Liu, C. Li and C.H. Chen, *Electrochim. Acta*, 2010, **55**, 2384.

29 K. Edström,T. Gustafsson and J.O. Thomas, *Electrochim. Acta*, 2004, **50**, 397.

30 L. Yang, M. Takahashi and B. Wang, *Electrochim. Acta*, 2006, **51**, 3228.

31 C.K. Chan, R. Ruffo, S. S. Hong and Y. Cui, *J. Power Sources*, 2009, **189**, 1132.

32 J.-T. Li, J. Swiatowska, A. Seyeux, L. Huang, V. Maurice, S.-G.Sun and P. Marcus, *J. Power Sources*, 2010, **195**, 8251.

33 A. T. Appapillai , A. N. Mansour , J. Cho and Y. S. Horn, *Chem. Mater.*, 2007, **19**, 5748.

34 S. Verdier, L. E. Ouatani, R. Dedryvère, F. Bonhomme, P. Biensan and D. Gonbeau, *J. Electrochem. Soc.*, 2007, **154**, A1088.

35 R.M. Jaeger, H. Kuhlenbeck, H.-J. Freund, M. Wuttig, W. Hoffmann, R. Franchy and H. Ibach, *Surf. Sci.*, 1991, **259**, 235.

36 K. S. Kim, *Phys. Rev. B*, 1975, **11**, 2177.

37 L. Dahéron, R. Dedryvère, H. Martinez, M. Ménétrier, C. Denage, C. Delmas and D. Gonbeau, *Chem. Mater.*, 2008, **20**, 583.

38 M. K. Devaraju, D. Rangappa and I. Honma, *Electrochim. Acta*, 2012, **85**, 548.

39 L. Tan, Z. Luo, H. Liu and Y. Yu, *J. Alloys Compd.*, 2010, **502**, 407.

40 M. Nagahama, N Hasegawa and S. Okada, *J. Electrochem. Soc.*, 2010, **157**, A748.

41 M. Herstedt, D.P. Abraham, J.B. Kerr and K. Edström, *Electrochim. Acta*, 2004, **49**, 5097.

42 J. Liu, N. Liu, D. Liu, Y. Bai, L. Shi, Z. Wang, L. Chen, V. Hennige and A. Schuch, *J. Electrochem. Soc.*, 2007, **154**, A55.

43 A. Lippitz, O. Boese, E. Kemnitz and W. E. S. Unger, *Surf. Sci. Spectra*, 2001, **8**, 1.

Table 1: Lithium ion diffusion coefficient of uncoated and Al_2O_3 coated Li_2CoPO_4F samples.

Li_2CoPO_4F sample	**Lithium ion diffusion coefficient (x 10^{-9} cm^2 s^{-1})**
Uncoated	5.13
1 wt% Al_2O_3	12.48
3 wt% Al_2O_3	8.69
5 wt% Al_2O_3	4.85

Figure captions

Figure 1. (a) X-ray diffraction patterns and (b) the corresponding FTIR spectra of as prepared Li_2CoPO_4F cathode materials with and without Al_2O_3 coating.

Figure 2. SEM images of (a) uncoated, (b) 1 wt%, (c) 3 wt%, and (d) 5 wt% Al_2O_3 coated Li_2CoPO_4F cathode materials. TEM images (scale: 10 nm) of uncoated and 1 wt% Al_2O_3 coated samples were given as inset in respective SEM images.

Figure 3. Initial charge/discharge curves of uncoated and Al_2O_3 coated Li_2CoPO_4F cathode materials at C/12 rate.

Figure 4. Evolution of charge/discharge curves of uncoated and Al_2O_3 coated Li_2CoPO_4F cathode materials at C/2 rate at (a) the first cycle, (b) the tenth cycle, and (c) the corresponding discharge capacity *vs*. cycle number results.

Figure 5. Cyclic Voltammogram of uncoated and Al_2O_3 coated Li_2CoPO_4F cathode materials between 2 and 5.1V at 0.1 mV s^{-1}. The magnified reduction peaks marked with a box is given as inset.

Figure 6. Electrochemical impedance spectroscopy of fresh cell between 100 kHz and 100 mHz frequency. The equivalent circuit used for fitting was given as inset with lines representing fitted data and symbols corresponding to experimental data.

Figure 7. (a) Al 2p, Co3p and Li 1s, (b) Co 2p, (c) O 1s, (d) P 2p and (e) F 1s spectral lines obtained from X-ray photoemission spectroscopy for the tested samples.

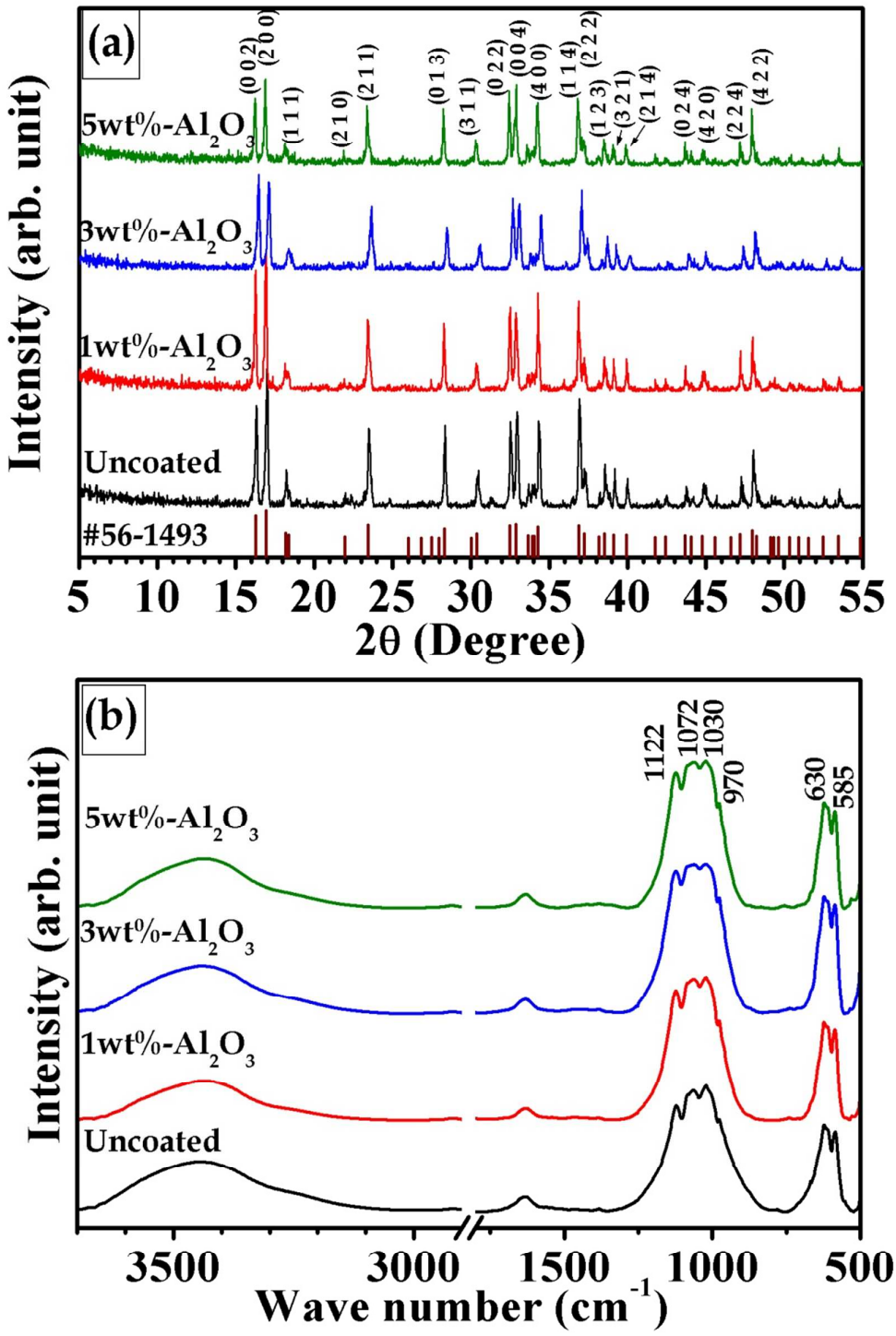

Y.S. Lee *et al.* Fig. 1

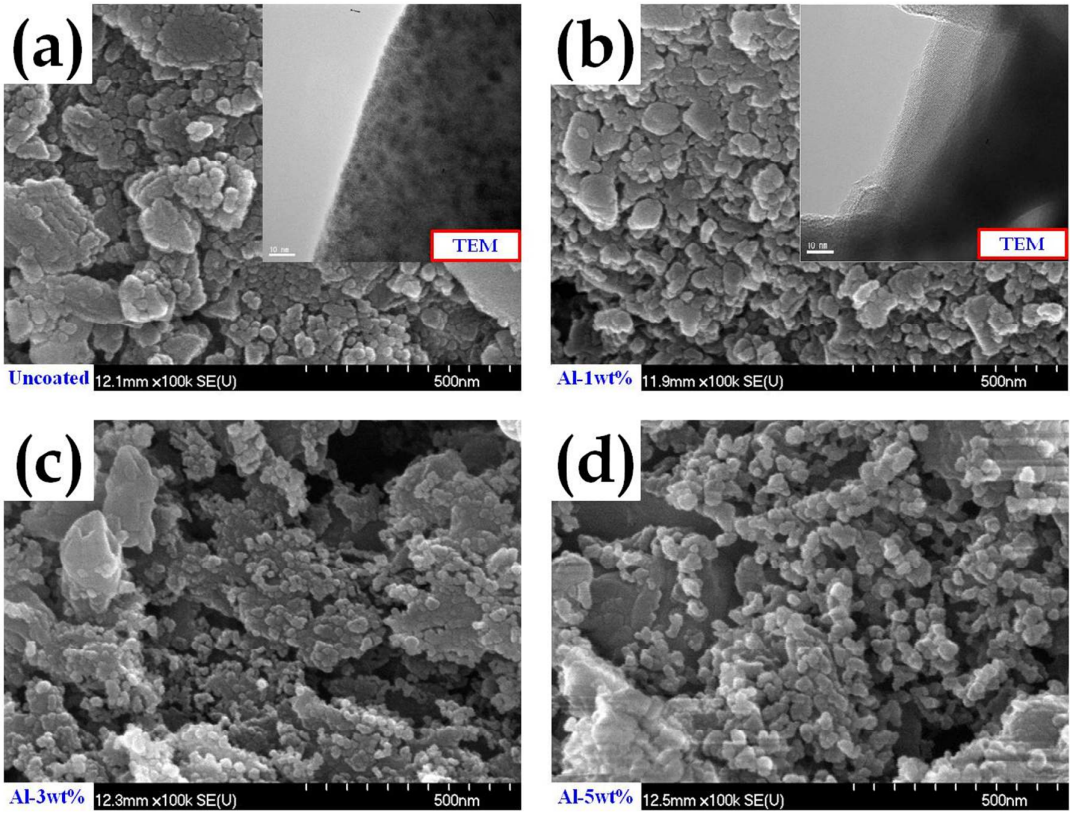

Y.S. Lee *et al.* Fig. 2

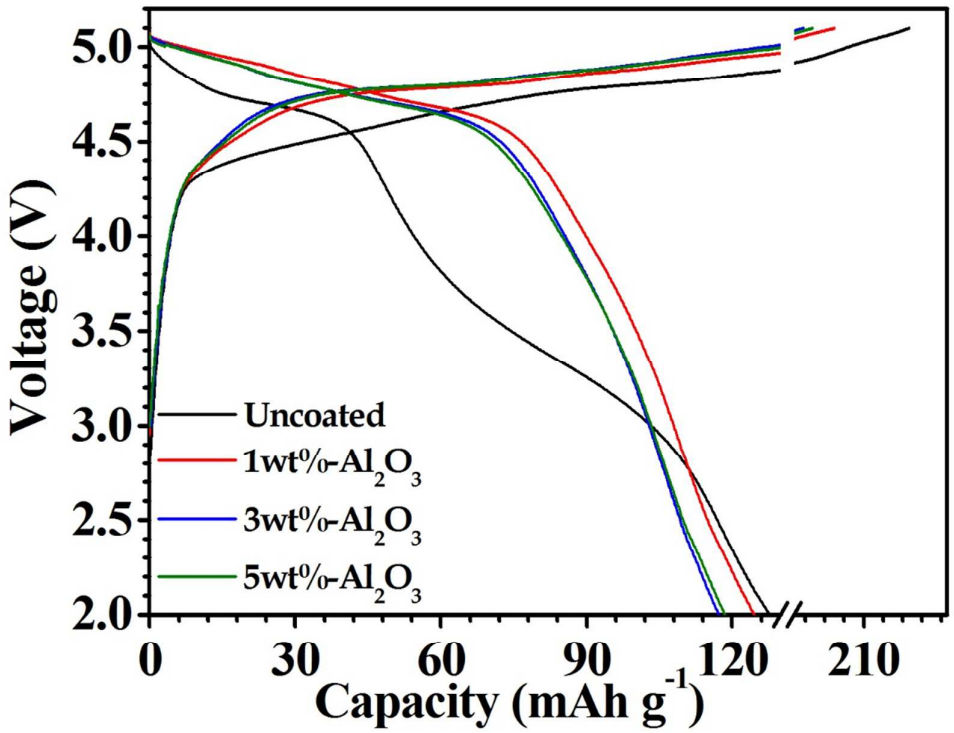

Y.S. Lee *et al.* Fig. 3

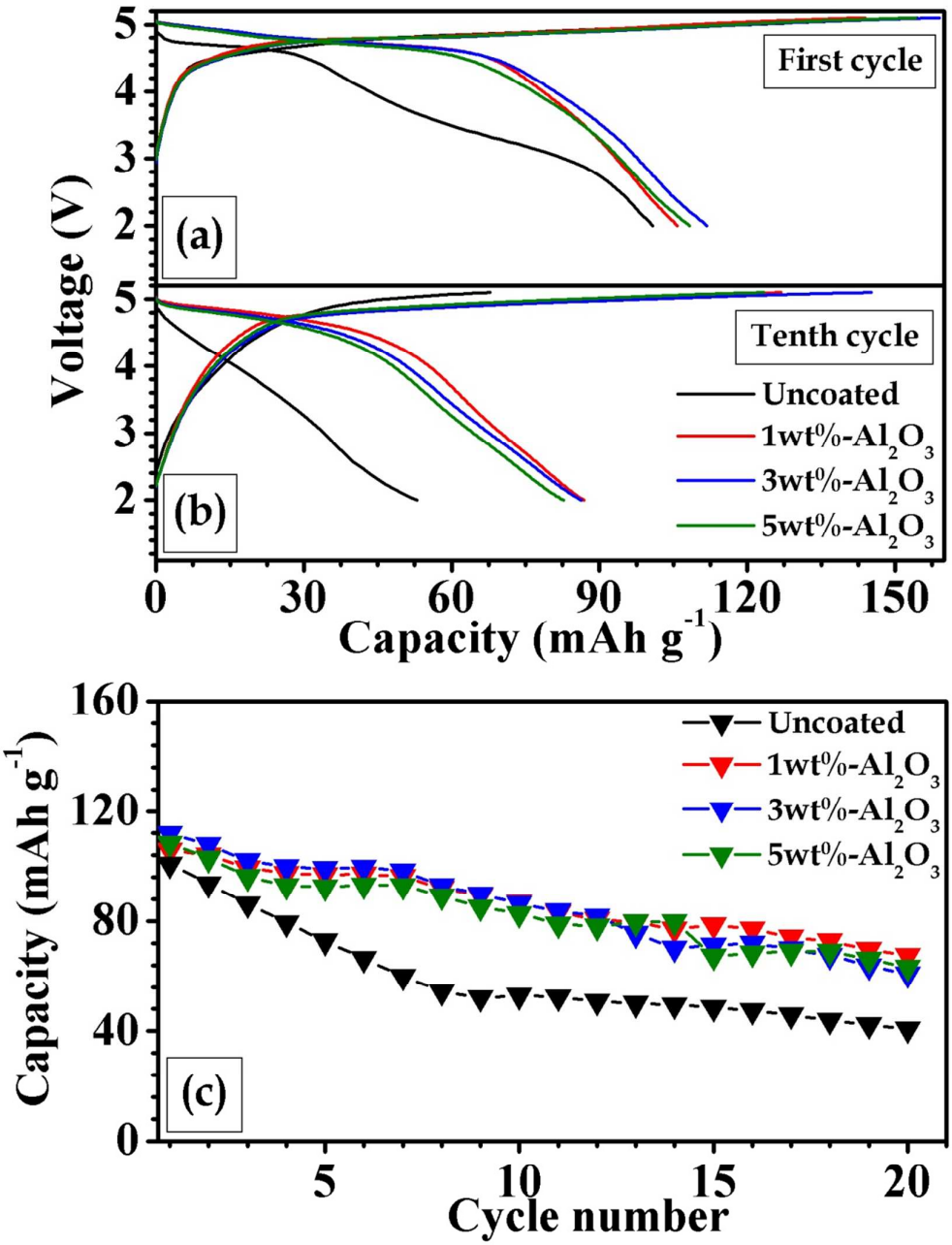

Y.S. Lee *et al.* Fig. 4

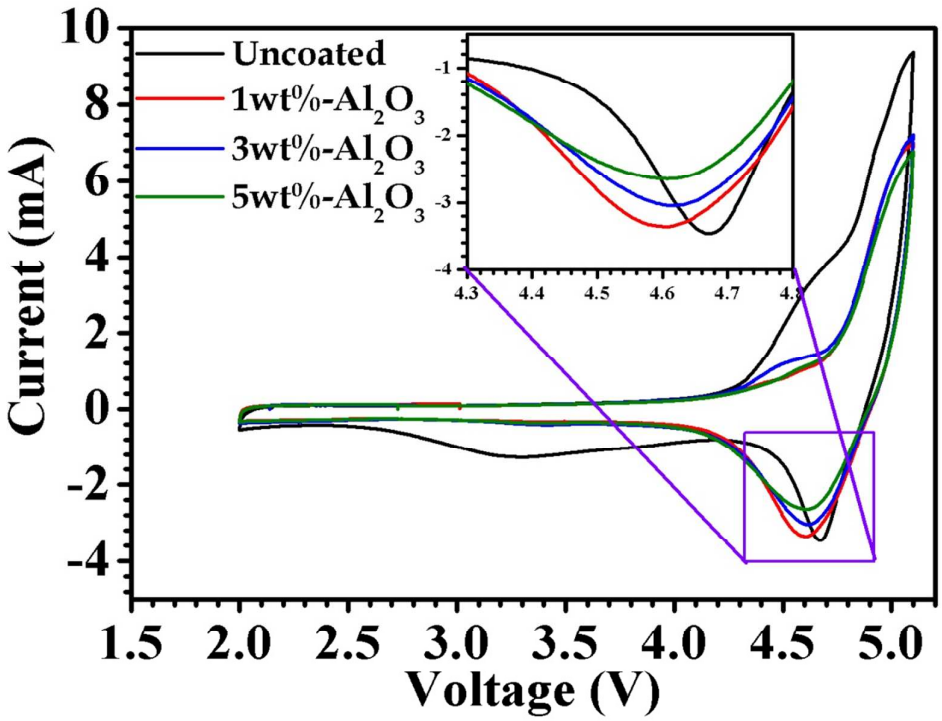

Y.S. Lee *et al.* Fig. 5

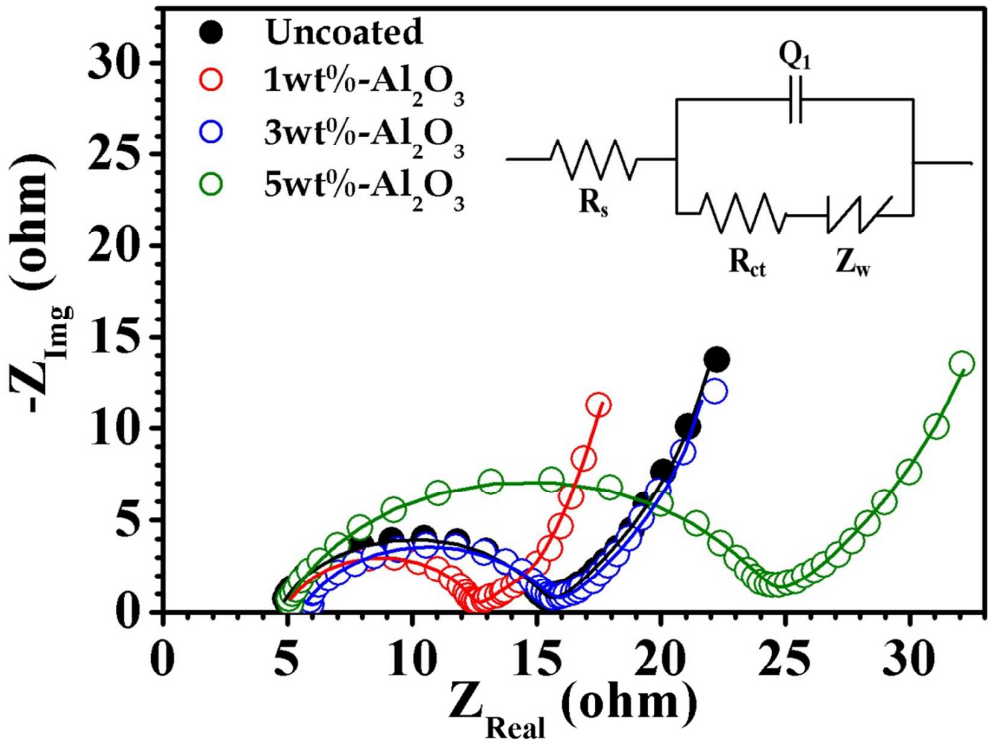

Y.S. Lee *et al.* Fig. 6

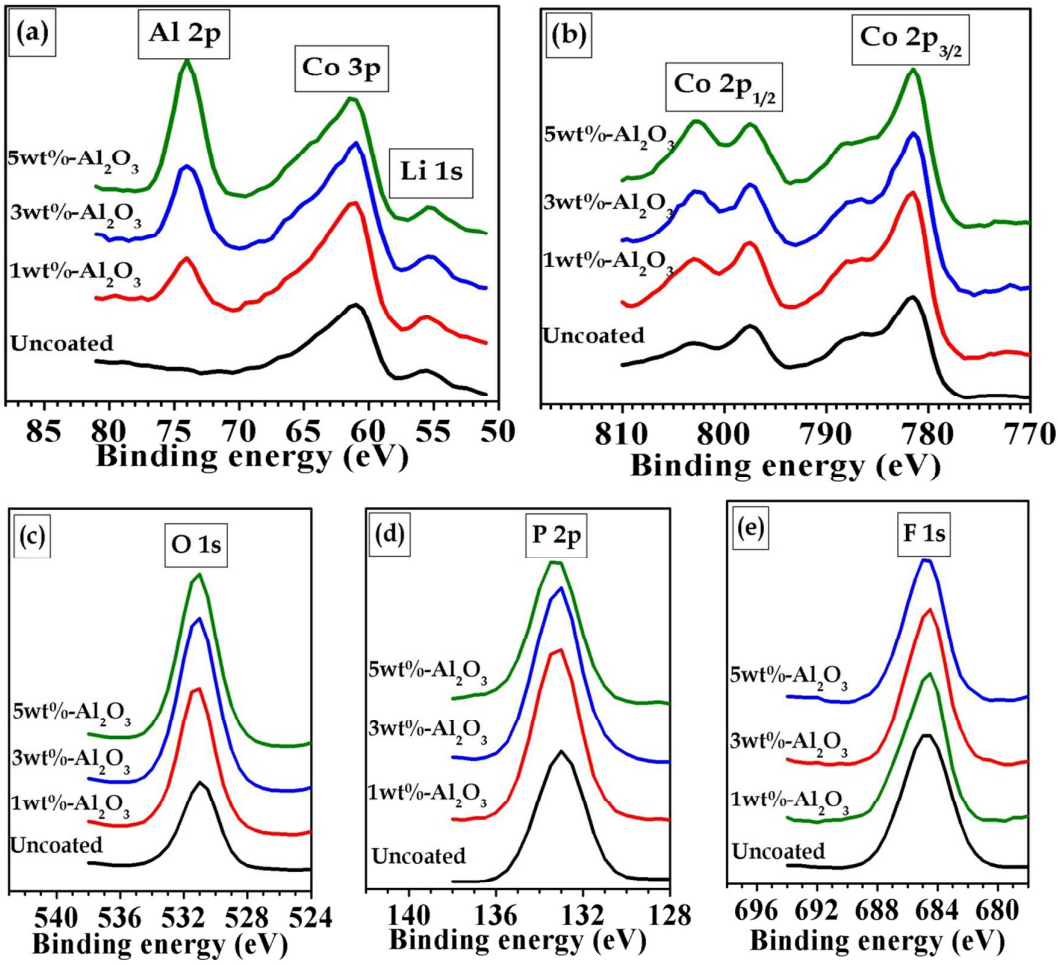

Y.S. Lee *et al.* Fig. 7